

Torus models for obscuration in type 2 AGN

Thomas Beckert¹, Wolfgang J. Duschl², and Bernd Vollmer³

¹ Max-Planck-Institut für Radioastronomie, Auf dem Hügel 69, 53121 Bonn, Germany

² Institut für Theoretische Astrophysik der Universität Heidelberg, Tiergartenstraße 15, 69121 Heidelberg, Germany

³ CDS, Observatoire astronomique de Strasbourg, UMR 7550, 11 rue de l'université, 67000 Strasbourg, France

Abstract. We discuss a clumpy model of obscuring dusty tori around AGN. Cloud-cloud collisions lead to an effective viscosity and a geometrically thick accretion disk, which has the required properties of a torus. Accretion in the combined gravitational potential of central black hole and stellar cluster generates free energy, which is dissipated in collisions, and maintains the thickness of the torus. A quantitative treatment for the torus in the prototypical Seyfert 2 nucleus of NGC 1068 together with a radiative transfer calculation for NIR re-emission from the torus is presented.

1 Introduction: Dusty tori in the unified model of AGN

Starting with the interpretation of spectropolarimetry of NGC 1068 by Antonucci & Miller [1,2], the difference between type 1 and type 2 AGN is attributed to aspect-angle-dependent obscuration. The central continuum source is thought to be surrounded by a dusty molecular gas distribution, which is flattened by rotation into a torus or thick disk. The simplest unification scheme assumes that all Seyfert 2 nuclei harbor a Seyfert 1 core, so that the ratio of type 1s to 2s measures the thickness of the torus. Present estimates range from 1:4 [3] to 1:1 [4] when selected in the mid-infrared. The torus should therefore have a thickness $H/R \sim 1$.

For more than a decade, clumpy models for the circumnuclear torus have been discussed [5]. It was recognized early on that dust will only survive in distinct clouds, which are embedded in the inter-cloud medium of the geometrically thick torus. This idea was nonetheless not included in the following radiative transfer calculations [6–9] of dust emission from these tori. Only recently, Nenkova et al. [10] developed a scheme which uses the clumpiness of the torus for an approximative and statistical calculation of the thermal IR-emission from clouds, which are individually optically thick $\tau_V > 40$. This approach resolved some of the problems with earlier radiative transfer calculations. The toroidal distribution of atomic and molecular material is also inferred from observed HI absorption and H₂ emission, for example in the nucleus of NGC 4151 [11].

In two papers [12,13] we studied the consequences of the proposed clumpiness. It turns out that a scenario with distinct, quasi-stable clouds, which experience frequent cloud-cloud collisions, is unavoidable for geometrically thick torus. In

in this paper we emphasize the importance of cloud collisions and present the results of radiative transfer calculations for the torus in NGC 1068.

2 Dusty clouds in the torus

Cold, molecular and dusty clouds are the basic constituents of an accretion scenario of the torus. In spite of the complexity of their internal physics, we regard them as spherical clouds, which are sufficiently described by their radius r_{Cl} and internal sound speed c_s . The clouds must be self-gravitating to prevent dissolving in the inter cloud medium, which implies that the clouds free-fall time and the sound crossing time are approximately equal. This determines the volume filling factor

$$\phi_V = \frac{32G\rho_0 r_{\text{Cl}}^2}{3\pi c_s^2} \quad (1)$$

of clouds, where $\rho_0 = \phi_V \rho_{\text{Cl}}$ is the mean mass density in the torus and ρ_{Cl} the density of individual clouds. The most important parameter of the torus in radiative transfer calculations is the vertical optical depth for intercepting a cloud

$$\tau = \int dz \tilde{l}_{\text{coll}}^{-1} = \xi \frac{H}{l_{\text{coll}}} , \quad (2)$$

where l_{coll} is the mean free path in the torus midplane (\tilde{l}_{coll} is the local value) and ξ is the coefficient of the linear relation between ρ_0 , pressure scale height H , and surface density $\Sigma = \xi \rho_0 H$, which follows from the vertical integration of the density. The radius r_{Cl} of clouds can then be expressed as a function of τ , c_s , and Σ .

The mean free path is likely to be dominated by the largest clouds present. These clouds are more affected by tidal shear than smaller ones, which sets an upper limit to the possible cloud sizes. We expect that clouds accumulate at the shear limit when they experience increasing tidal forces while being accreted to the center. The upper limit is

$$r_{\text{Cl}} \leq \frac{\pi}{\sqrt{8}} \frac{c_s}{\Omega} . \quad (3)$$

This is also a lower limit to the surface density

$$\Sigma \geq \frac{\tau}{\sqrt{8}} \frac{M(R)}{R^2} \frac{c_s}{v_\phi} . \quad (4)$$

Here $M(R)$ is the total enclosed mass in stars and black hole at radius R and v_ϕ is the Keplerian circular velocity at that position. Both mass and optical depth will be dominated by the largest clouds and the right side of (4) will be a good measure of the true surface density. This implies a one to one correspondence between Σ and τ . For the mass of individual clouds

$$M_{\text{Cl}} \leq M(R) \frac{\pi^3}{16\sqrt{2}} \frac{c_s^3}{v_\phi^3} \quad (5)$$

we find an upper limit, which is much smaller than the typical mass of molecular clouds in the ISM of normal galaxies. At a radius of 2 pc with an enclosed mass of $10^7 M_\odot$ and an internal sound speed against gravitational cloud collapse of $c_s = 2$ km/s gives a largest possible mass of $35 M_\odot$. Contrary to the cloud mass we find a lower limit for the hydrogen column density through an individual cloud

$$N_H \geq \frac{M(R)}{\mu m_H} \frac{c_s}{\sqrt{8} R^2 v_\phi} \quad (6)$$

which is about 10^{24} cm $^{-2}$ in the environment close to the sublimation radius parameterized above.

For the distribution of clouds in the torus we assume hydrostatic equilibrium for the vertical stratification. In [13] we used a modified isothermal distribution function of cloud velocities in an external potential, which includes a cut-off scale height x_H at which the density drops to zero. This leaves room for a wide polar funnel or an outflow cavity. We consider only cases, where the cut-off height is larger than the pressure scale height H . An example for the case of NGC 1068 is shown in Fig. 1. The radial structure is derived from the stationary accretion scenario described below.

3 Cloud collisions and accretion

The unified model of AGN requires at least $\tau \sim 1$ for obscuration of the AGN for line of sights through the torus. As τ is also a dimensionless collision frequency $\tau \sim \omega_c/\Omega$, this implies that cloud-cloud collisions are frequent in a torus. For anisotropic velocity dispersions of clouds Goldreich & Tremaine [14] derived an effective viscosity

$$\nu = \frac{\tau}{1 + \tau^2} \frac{\sigma^2}{\Omega} \quad (7)$$

for angular momentum redistribution¹. The required anisotropy can be determined self-consistently for thin accretion disks and we use this limit also for the torus.

Because in our scenario clouds in a torus are quasi-stable and only created or destroyed in cloud collisions, the momentum transfer from supernovae and stellar winds is inefficient for maintaining a large velocity dispersion of clouds. Accretion in the gravitational potential due to cloud collisions generate the free energy to balance collisional dissipation.

Like in ordinary accretion disks, the effective viscosity from (7) allows mass to be accreted towards the black hole. The conservation law of angular momentum for the torus clouds with a viscous torque can be integrated once for stationary accretion

$$\nu \Sigma R^3 \frac{\partial \Omega}{\partial r} - \nu_i \Sigma_i R_i^3 \left(\frac{\partial \Omega}{\partial r} \right) \Big|_{r=R_i} = - \frac{\dot{M}}{2\pi} R^2 \Omega \left(1 - \frac{\Omega_i}{\Omega} \left(\frac{R_i}{R} \right)^2 \right). \quad (8)$$

¹ The enhanced viscosity due to collective effects described by Wisdom & Tremaine [15] is unimportant for geometrically thick disks or tori with $\Phi_V \ll 1$.

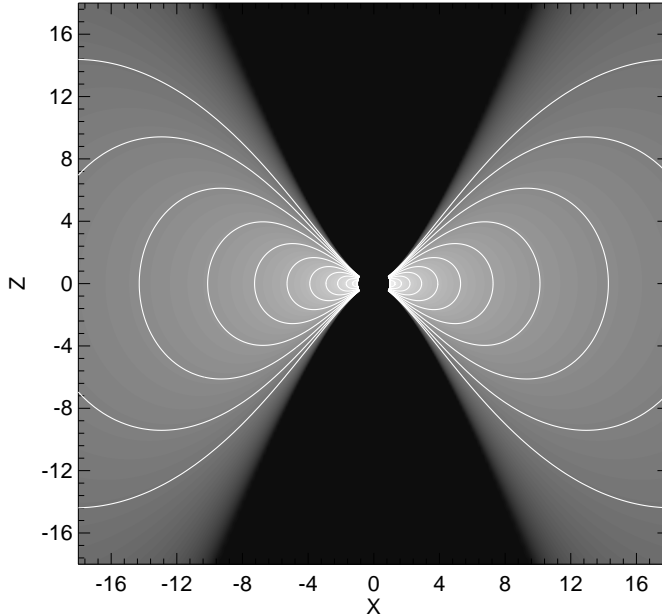


Fig. 1. Meridional cut through the probability density distribution of finding a dusty cloud in the torus. The distribution leaves room for an outflow along the polar axis and is derived from the model of Beckert & Duschl [13]. The spatial scale is in units of the dust sublimation radius. The mean number of clouds along a line of sight to the center drops below 1 for angles larger than 40° from the midplane ($Z = 0$).

Special attention must be paid to the inner boundary at R_i (index i). This boundary will be at the sublimation radius for dust ($R \sim 1$ pc), where neither torque nor shear will vanish. In addition the torque at the inner boundary is most likely not well described by the viscosity (7). Here \dot{M} is the total mass accretion rate, which we assume to be constant at all radii throughout the torus. The outer boundary of our model is determined by the feeding process. The mass supply can be either a steady inflow driven by circumnuclear starformation, discrete interactions with GMCs coming from large radii, or an inflow created by bars in the galactic potential.

In cloud-cloud collisions a fraction $\frac{1}{2}(1 - \epsilon^2)$ of the average relative kinetic energy of clouds is dissipated, where ϵ is the coefficient of restitution, which approaches 1 for elastic collisions. We use ϵ to parameterize cloud collisions and ignore the possibly more complex momentum redistribution in actual collisions. The energy dissipation appears as a sink term in the energy balance. For thin accretion disks with $\tau \sim 1$ we find $\epsilon > 0.8$, which is uncomfortably large. Smaller values of ϵ are possible in geometrically thick tori, because energy advection can balance the increased dissipation in collisions. For a given set of parameters

$(\epsilon, \dot{M}, M(R))$ the surprising result is that tori with high accretion rates are geometrically thick $H/R \sim \sqrt{2R\dot{M}/(c_s M(R))}$ in spite of the smaller ϵ of collisions. The elasticity, which leads to reasonably thick tori have ϵ in the range 0.2–0.6, which might be provided by magnetic fields in the clouds.

4 The Torus in NGC 1068

For a detailed model of the torus one needs to know the mass distribution in the center. For the case of NGC 1068 we collected the data in [13]. Some of the observed H₂O-maser spots [16] around the radio core component S1 [17] trace a rotating disk or ring. The maser velocities appear inconsistent with Keplerian rotation around a central point mass. The rotation profile can be due to a massive disk [18], but we follow [19] and find a model with a black hole mass of $1.2 \cdot 10^7 M_\odot$ and a strongly concentrated stellar cluster with $\rho_* \propto R^{-\alpha}$ at large radii, a core radius of 0.32 pc and a core density of $\rho_{*,c} = 5.25 \cdot 10^6 M_\odot \text{ pc}^{-3}$. Core radius and density are comparable to the nuclear stellar cluster in the center of our Galaxy [20]. The observational data from 0.3'' to 4'' from the nucleus are consistent with

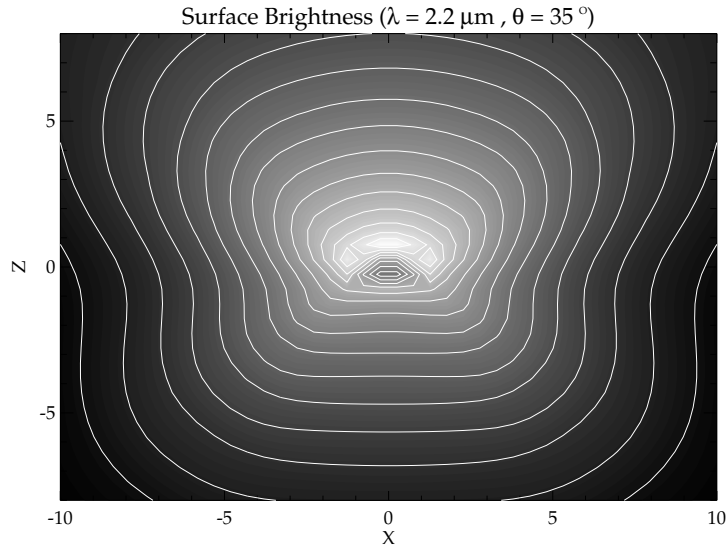


Fig. 2. K-band brightness distribution of our radiative transfer calculations based on the method of Nenkova et al. [10] and the scenario of Beckert & Duschl [13] for an inclination of 35° from the midplane. The spatial scale is in units of the dust sublimation radius. The contour scale of the surface brightness is logarithmic with a dynamic range of 2^{14} .

this mass distribution. The central cluster extends out to 250 pc and the dusty torus lives in the gravitational potential of this cluster.

With the mass distribution, the model for individual clouds, and the cloud density distribution from Fig. 1 we performed radiative transfer calculations based on the method of Nenkova et al. [10]. An example of the surface brightness distribution is shown in Fig. 2. The simulation demonstrate that the observed core component in Speckle images [21] in the NIR indeed measures the size of the sublimation radius to $R = 1 \pm 0.4$ pc.

5 Conclusions

We described a dynamical approach to the radial and vertical structure of a clumpy torus around an AGN following the ideas of Krolik & Begelman [5] and Vollmer et al. [12]. The vertical thickness is derived from an accretion scenario for a geometrically thick torus, which is based on cloud-cloud collisions. The inferred mass accretion rates for scale heights $H > 0.5R$ in the torus are larger than the Eddington rate for the central black hole and the model requires massive outflows from within the sublimation radius for dust. It is found that along typical lines of sight to the center (for angles $< 45^\circ$ w.r.t. the torus midplane) between one and ten clouds on average obscure the AGN. Only a small fraction of the mass accreted through the torus eventually reaches the black hole but is sufficient to generate the ionizing luminosity. An in depth analysis of cloud collisions in the environment of an AGN is required to test our model assumptions for ϵ and the structure of individual clouds.

References

1. J. S. Miller, R. R. J. Antonucci: ApJ, **271**, L7 (1983)
2. R. R. J. Antonucci, J. S. Miller: ApJ, **297**, 621 (1985)
3. R. Maiolino, G. H. Rieke: ApJ, **454**, 95 (1995)
4. M. Lacy, L. J. Storrie-Lombardi, A. Sajina et al.: ApJS, **154**, 166 (2004)
5. J. H. Krolik M. C. Begelman: ApJ **329**, 702 (1988)
6. E. A. Pier, J. H. Krolik: ApJ, **401**, 99 (1992)
7. E. A. Pier, J. H. Krolik: ApJ, **418**, 673 (1993)
8. G. L. Granato, L. Danese: MNRAS, **268**, 235 (1994)
9. A. Efstatthiou, M. Rowan-Robinson: MNRAS, **273**, 649 (1995)
10. M. Nenkova, Ž. Ivezić, M. Elitzur: ApJ **570**, L9 (2002)
11. C. G. Mundell, J. M. Wrobel, A. Pedlar, J. F. Gallimore: ApJ, **583**, 192 (2003)
12. B. Vollmer, T. Beckert, W. J. Duschl: A&A **413**, 949 (2004)
13. T. Beckert, W. J. Duschl: A&A **426**, 445 (2004)
14. P. Goldreich, S. Tremaine: Icarus, **34**, 227 (1978)
15. J. Wisdom, S. Tremaine: AJ, **95**, 925 (1988)
16. L. J. Greenhill, C. R. Gwinn: Astrophysics and Space Science, **248**, 261 (1997)
17. J. F. Gallimore, S. A. Baum, C. P. O'Dea: ApJ, **613**, 794 (2004)
18. J.-M. Huré: A&A, **395**, L21 (2002)
19. P. Kumar: ApJ, **519**, 599 (1999)
20. R. Schödel, T. Ott, R. Genzel et al.: ApJ, **596**, 1015 (2003)
21. G. Weigelt, M. Wittkowski, Y. Y. Balega et al.: A&A, **425**, 77 (2004)